Chemistry and Physics of Lipids 245 (2022) 105205

Contents lists available at ScienceDirect

Chemistry and Physics of Lipids

journal homepage: www.elsevier.com/locate/chemphyslip

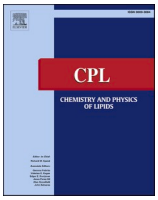

Research paper

Influence of ceramide on lipid domain stability studied with small-angle neutron scattering: The role of acyl chain length and unsaturation

Mitchell DiPasquale [a], Tye G. Deering [b], Dhimant Desai [c], Arun K. Sharma [c], Shantu Amin [c], Todd E. Fox [b], Mark Kester [b,d], John Katsaras [e,f,g,*], Drew Marquardt [a,h,**], Frederick A. Heberle [i,***]

[a] Department of Chemistry and Biochemistry, University of Windsor, Windsor N9B 3P4, ON, Canada
[b] Department of Pharmacology, University of Virginia, Charlottesville 22908, VA, USA
[c] Department of Pharmacology, Penn State University, University Park 16801, PA, USA
[d] Department of Molecular Physiology and Biophysics, University of Virginia, Charlottesville 22908, VA, USA
[e] Neutron Scattering Division, Oak Ridge National Laboratory, Oak Ridge 37831, TN, USA
[f] Joint Institute for Neutron Sciences, Oak Ridge National Laboratory, Oak Ridge 37831, TN, USA
[g] Department of Physics and Astronomy, University of Tennessee, Knoxville 37996, TN, USA
[h] Department of Physics, University of Windsor, Windsor N9B 3P4, ON, Canada
[i] Department of Chemistry, University of Tennessee, Knoxville 37996, TN, USA

ARTICLE INFO

Keywords:
Ceramide
Diacylglycerol
Lipid rafts
Lipid domains
Small-angle neutron scattering

ABSTRACT

Ceramides and diacylglycerols are groups of lipids capable of nucleating and stabilizing ordered lipid domains, structures that have been implicated in a range of biological processes. Previous studies have used fluorescence reporter molecules to explore the influence of ceramide acyl chain structure on sphingolipid-rich ordered phases. Here, we use small-angle neutron scattering (SANS) to examine the ability of ceramides and diacylglycerols to promote lipid domain formation in the well-characterized domain-forming mixture DPPC/DOPC/cholesterol. SANS is a powerful, probe-free technique for interrogating membrane heterogeneity, as it is differentially sensitive to hydrogen's stable isotopes protium and deuterium. Specifically, neutron contrast is generated through selective deuteration of lipid species, thus enabling the detection of nanoscopic domains enriched in deuterated saturated lipids dispersed in a matrix of protiated unsaturated lipids. Using large unilamellar vesicles, we found that upon replacing 10 mol% DPPC with either C16:0 or C18:0 ceramide, or 16:0 diacylglycerol (dag), lipid domains persisted to higher temperatures. However, when DPPC was replaced with short chain (C6:0 or C12:0) or very long chain (C24:0) ceramides, or ceramides with unsaturated acyl chains of any length (C6:1(3), C6:1(5), C18:1, and C24:1), as well as C18:1-dag, lipid domains were destabilized, melting at lower temperatures than those in the DPPC/DOPC/cholesterol system. These results show how ceramide acyl chain length and unsaturation influence lipid domains and have implications for how cell membranes might modify their function through the generation of different ceramide species.

1. Introduction

The liquid-ordered (L_o) membrane phase is a unique state of matter that arises from a preferential interaction between cholesterol and either sphingolipids or saturated phospholipids (Ipsen et al., 1987). In the presence of unsaturated phospholipids, L_o phases can coexist with disordered liquid (L_d) phases over a broad range of composition and temperature (Marsh, 1788; Heberle and Feigenson, 2011). The appearance of L_d+L_o phase separation in model membranes that mimic the composition of eukaryotic plasma membrane outer leaflets has generally helped shed light on observations of lipid rafts in living cells (Simons and Ikonen, 1997). In particular, rafts are thought to be ordered lipid domains enriched in cholesterol and sphingolipids that are stabilized by a network of hydrogen bonds (Slotte, 2016; Sodt et al., 2015). The small

* Corresponding author at: Neutron Scattering Division, Oak Ridge National Laboratory, Oak Ridge 37831, TN, USA
** Corresponding author at: Department of Chemistry and Biochemistry, University of Windsor, Windsor N9B 3P4, ON, Canada
*** Corresponding author.
E-mail addresses: katsarasj@ornl.gov (J. Katsaras), drew.marquardt@uwindsor.ca (D. Marquardt), fheberle@utk.edu (F.A. Heberle).

https://doi.org/10.1016/j.chemphyslip.2022.105205
Received 19 March 2022; Accepted 11 April 2022
Available online 26 April 2022
0009-3084/

(nanoscopic) size and transient lifetime of ordered domains in resting cells has fueled an ongoing debate regarding the physicochemical origins of membrane rafts (Levental et al., 2020). Whether these domains are a manifestation of L_d+L_o phase separation (Feigenson, 1863), critical fluctuations (Veatch, 2022), a microemulsion (Allender et al., 2020), or some other mechanism remains an open question.

Although the canonical raft models are understandably based on the most abundant classes of plasma membrane lipids (i.e., ternary mixtures of high-melting and low-melting phospholipids together with cholesterol), minor plasma membrane lipid components can have a profound influence on raft behavior. A prime example are ceramides, a diverse class of sphingolipid metabolites that are among the most hydrophobic biomolecules found in nature (Kolesnick et al., 2000). Similar to cholesterol, ceramides can selectively partition into ordered lipid phases to minimize their interaction with water (Wang and Silvius, 2003; Huang and Feigenson, 1999). As shown in Fig. 1A, the relatively small hydroxyl headgroup of ceramide, together with its sphingoid backbone and long acyl chains, produce a structure that is highly suited for interactions with ordered lipid domains. Under certain conditions, ceramides can reach concentrations of up to 10 mol% in ordered phases (Hannun, 1996) and may have a greater propensity than cholesterol to associate with ordered phases (Wang and Silvius, 2003; Ali et al., 2006). The association between ceramides and ordered lipid phases is known to stabilize lipid domains (Goñi and Alonso, 2009), but in turn excludes cholesterol from these domains (Grassmé et al., 2002; Zhang et al., 2009).

The complex interaction between ceramide, cholesterol, and other raft-forming lipids is becoming a topic of increasing interest, as an understanding of their physicochemical properties is of central importance for defining the potential biological roles of lipid rafts (Cremesti et al., 2002; Kinnunen et al., 1994). For example, ceramides have been shown to participate in a wide range of cellular processes taking place at the membrane, including protein function (Kolesnick et al., 2000), signaling (Mathias et al., 1998; Stancevic and Kolesnick, 2010), and cell apoptosis (Li et al., 2006; Huang et al., 2011; Pushkareva et al., 1995). Moreover, the differential tissue expression of various ceramide synthases points to different membrane behaviors associated with particular ceramide acyl chains (Laviad et al., 2008).

Several studies have found that ceramides can displace cholesterol from sphingolipid-rich ordered phases, essentially modifying membrane fluidity by forming ceramide-rich gel domains (Maula et al., 2015; Pinto et al., 2011; Nybond et al., 2005; Megha et al., 2007). In most of these studies, lipid phase behavior was interrogated through the use of fluorescent reporter molecules, which can in some cases, perturb the local membrane environment (Ackerman et al., 2013). In this work, we used small-angle neutron scattering (SANS), an essentially probe-free technique capable of detecting nanoscopic lipid domains (Pencer et al., 2007; Heberle et al., 2013). Specifically, we used SANS to report on the clustering of saturated lipids in the presence of different ceramide and diacylglycerol species. Diacylglycerols (Fig. 1B) are structurally similar to ceramides but lack the ability to hydrogen bond. We chose a glycerophospholipid-based lipid composition to reduce backbone hydrogen bonding, thus allowing us to better compare the effects of ceramide and diacylglycerol acyl chains. Our experimental strategy was to replace 10 mol% of the saturated lipid in the prototypical ternary domain-forming composition DPPC/DOPC/Chol (37.5/37.5/25) with various species of ceramide or diacylglycerol differing in fatty acid chain length and degree of unsaturation, resulting in a quaternary mixture with sufficient amounts of saturated lipid and cholesterol to inhibit the formation of ceramide-rich gel domains (Veatch and Keller, 2003; Boulgaropoulos et al., 2012; Castro et al., 2009; Pinto et al., 2013).

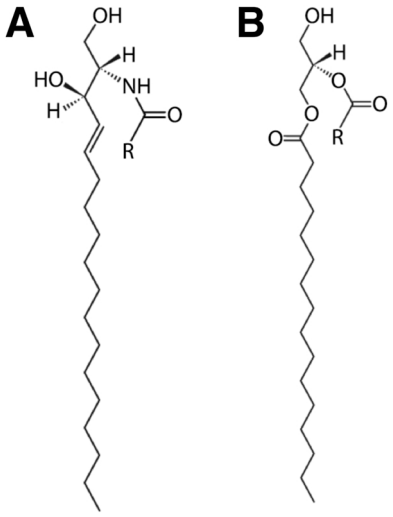

Fig. 1. Structures of (A) ceramide (cer) and (B) diacylglycerol (dag). In contrast to the glycerol backbone of phospholipids, the sphingoid backbone of ceramides is both a hydrogen bond donor and acceptor.

2. Results

We collected SANS data from extruded large unilamellar vesicle (LUV) samples in which the average neutron scattering length density (NSLD) of the lipid bilayer was matched to the surrounding water, but where the average NSLDs of the saturated and unsaturated lipid species were not matched to each other. In such a sample, any excess coherent scattering above the flat incoherent background is the result of a nonrandom lateral spatial arrangement of saturated and unsaturated lipids (i.e., lipid clustering) on length scales accessible to the SANS technique (i.e., domains of greater than $\approx$ 5 nm) (Heberle et al., 2013). We compared samples doped with protiated ceramide (cer) or diacylglycerol (dag) species to a baseline mixture devoid of the dopant. The baseline composition was DPPC/DOPC/Chol (37.5/37.5/25, by mole fraction), a well-characterized mixture that phase-separates into coexisting liquid-ordered (saturated-rich, L_o) and liquid-disordered (unsaturated-rich, L_d) domains below $\approx$ 32 °C (Veatch and Keller, 2003). In each sample, 10 mol% of the saturated lipid DPPC was replaced by a cer or dag of different acyl chain length and/or degree of unsaturation, while keeping the overall average NSLD of the mixture constant (Heberle et al., 2013). Using this experimental approach, we maintained a constant molar ratio of cholesterol, cer/dag, and high-melting temperature lipid, which has been shown to be a critical modulator of phase behavior in ceramide containing mixtures (Pinto et al., 2013; Castro et al., 2009; Silva et al., 2009). The use of DPPC (rather than sphingomyelin) in the baseline mixture avoids bias toward domain stabilization by hydrogen bonding between the sphingoid backbone of ceramide and that of sphingomyelin lipids (Maula et al., 2015; Jaikishan and Slotte, 2013).

Previous work using a sphingolipid-based, raft-forming ternary mixture suggested that some ceramides with long acyl chains can form a ceramide-rich gel (L_β) phase at low cholesterol concentrations (Castro et al., 2009). We used a cholesterol concentration (25 mol%) that is significantly higher than the ceramide concentration (10 mol%) to minimize the possibility of L_β formation. Additionally, because the ceramide and diacylglycerol species are protiated, any induced gel domains would have an NSLD similar to the protiated bulk phase, and thus changes in scattering can be directly correlated to changes in the clustering of deuterated DPPC-rich L_o phase.

Fig. 2 shows SANS curves for the ceramide-free baseline sample as well as samples where 10 mol% of the DPPC was replaced by either C18:0-cer or C18:1-cer. At 15 °C, the ceramide-free sample (blue curve) shows a characteristic peak at ≈ 0.005 Å^{-1} resulting from lateral segregation of the deuterated and protiated lipid components, consistent with previous observations (Pencer et al., 2005). The coherent scattering peak is markedly reduced upon raising the temperature to 25 °C, and is completely lost by 35 °C, suggesting a well-mixed fluid bilayer, consistent with published phase diagrams for this mixture (Veatch and Keller,

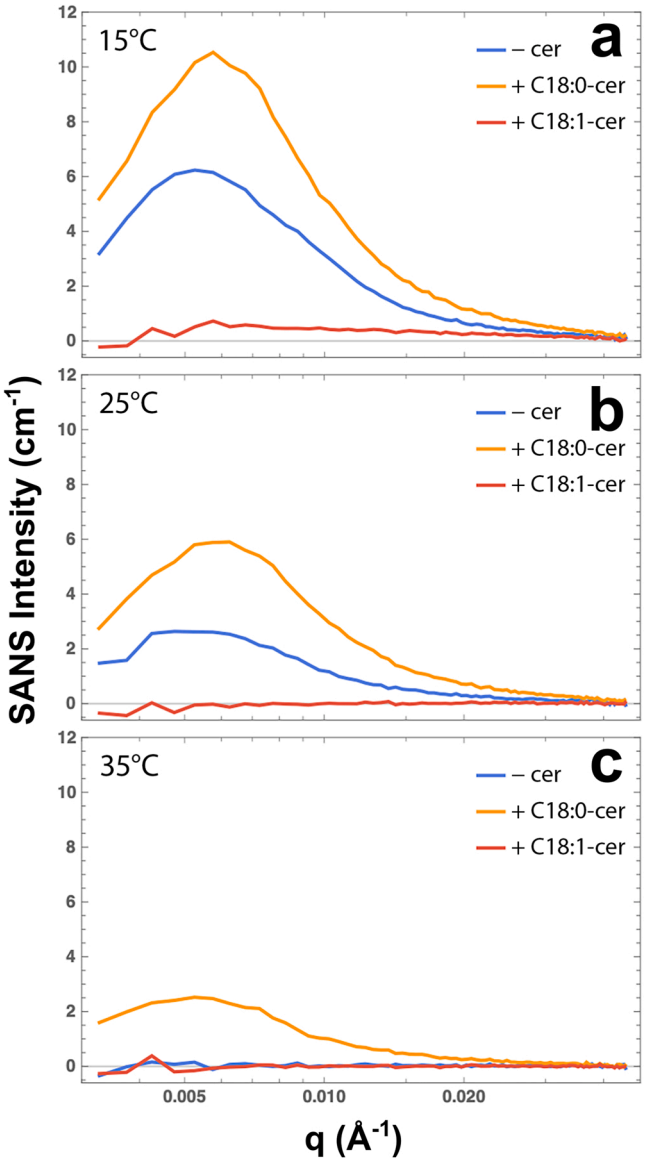

Fig. 2. SANS reveals the effects of membrane additives on domain stability. SANS data at 15 °C (a), 25 °C (b), and 35 °C (c) for the lipid mixture DPPC/DOPC/Chol 37.5/37.5/25 in the absence of ceramide (-cer, blue curve), or with 10 mol% of DPPC replaced by either C18:0-cer (orange curve), or C18:1-cer (red curve). C18:0-cer stabilizes domains as indicated by an increase in SANS intensity relative to the baseline, while C18:1-cer destabilizes them. Close to physiological temperature (c), C18:0-cer induces domain formation in the uniform baseline lipid mixture.

2003). Partial replacement of DPPC with C18:0-cer (orange curve) increases the scattering intensity relative to the baseline mixture at all temperatures, indicating that this lipid induces greater segregation of DPPC from the other lipids. In contrast, C18:1-cer (red curve) abolishes coherent scattering at all temperatures, suggesting that this lipid causes DPPC to mix with the other lipids.

To quantitatively compare the influence of the different ceramide species on lateral lipid heterogeneity, we calculated the Porod invariant, Q, from the SANS data as described in the Experimental Procedures. Given the contrast scheme, an increase (decrease) in Q reflects stronger (weaker) lateral segregation of saturated and unsaturated lipids, that is, a change in the propensity of the ordered lipid DPPC to cluster. Here and throughout, we use the shorthand language that increased Q corresponds to a dopant that stabilizes domains, while decreased Q corresponds to domain destabilization. Fig. 3 shows Q plotted against acyl

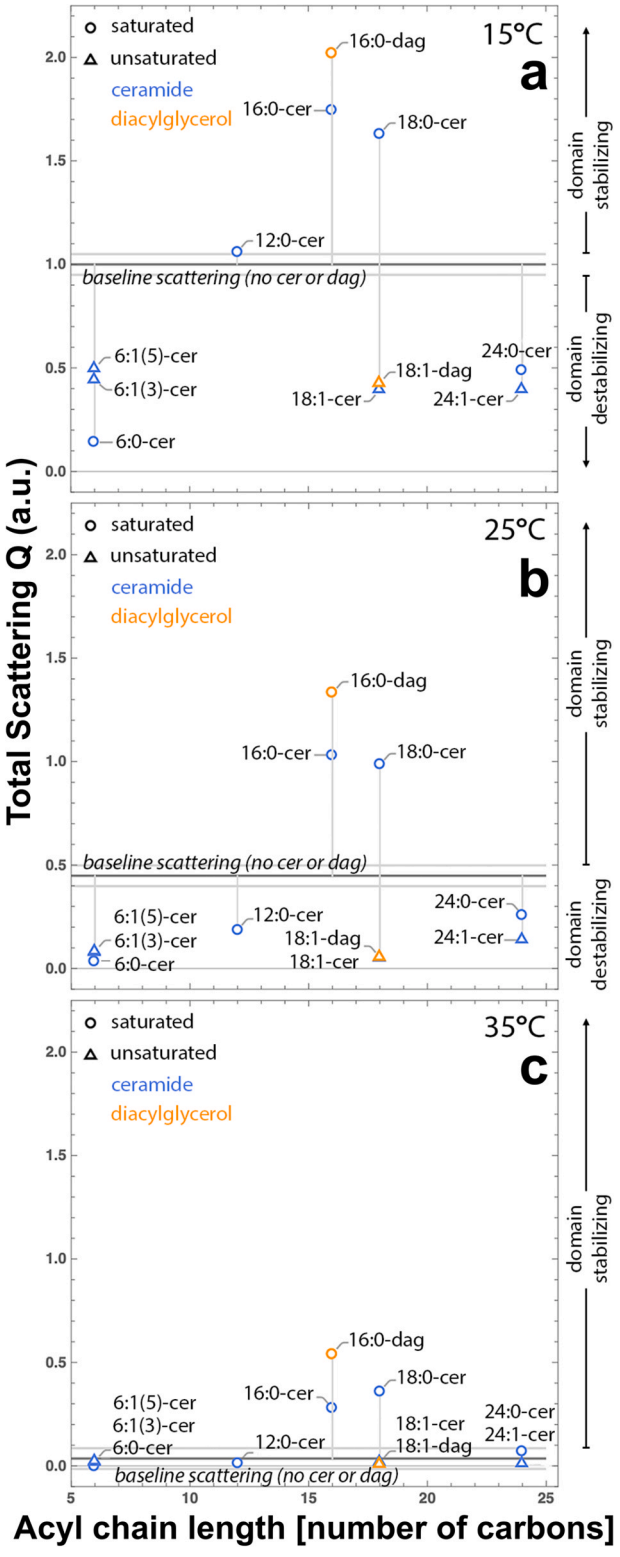

Fig. 3. Domain stabilization or destabilization by ceramide depends on the structure of its N-acyl chain. The normalized Porod invariant, Q, is correlated to the acyl chain length of different saturated and unsaturated (open circles and open triangles, respectively) ceramides and diacylglycerols (blue and orange, respectively) at (a) 15 °C, (b) 25 °C, and (c) 35 °C. Species above the horizontal black line stabilize domains relative to the baseline lipid mixture, while those below the line destabilize domains. The horizontal gray lines denote one standard deviation derived from replicate experiments of the baseline composition.

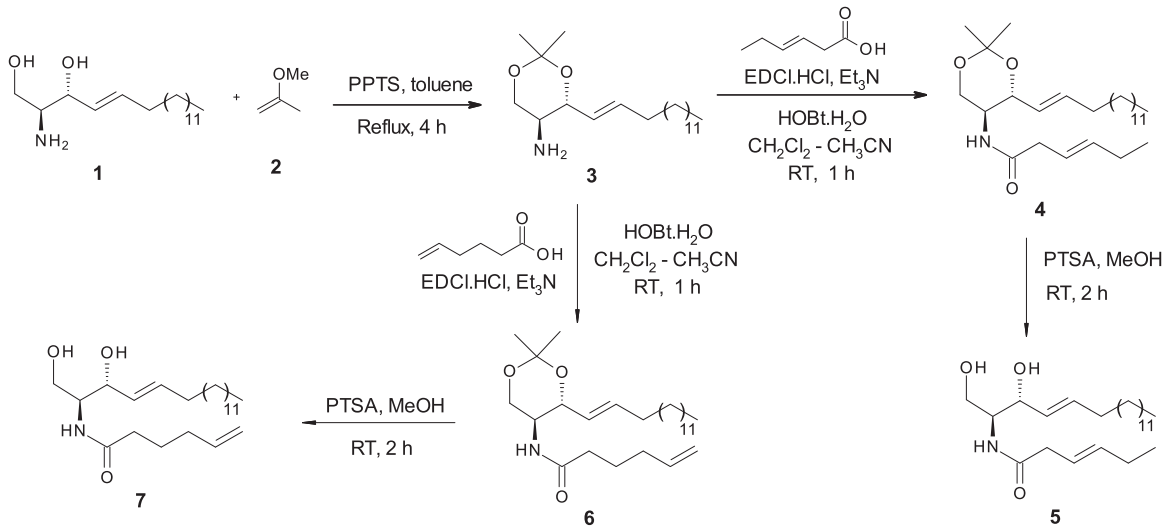

Fig. 4. Synthesis of C6:1-cer species.

chain length for various saturated and unsaturated (open circles and triangles, respectively) ceramides and diacylglycerols (blue and orange symbols, respectively) at (a) 15 °C, (b) 25 °C, and (c) 35 °C. Of the eleven species investigated, only three (i.e., C16:0-cer, C18:0-cer, and C16:0-dag) were found to stabilize domains and, as shown in Fig. 3c, induce domains in an otherwise uniform mixture at 35 °C. In contrast, domains were destabilized by dopants with short saturated chains (C6:0-cer and C12:0-cer), long saturated chains (C24:0-cer), or by an unsaturated chain of any length (C6:1-cer, C18:1-cer, C24:1-cer, and C18:1-dag). Fig. 4.

Considering only the ceramide species, the hierarchy for propensity to stabilize domains is as follows: C18:0 ≈ C16:0 > no ceramide ≈ C12:0 > C24:0 ≈ C24:1 ≈ C18:1 ≈ C6:1 > C6:0. At all temperatures studied, C6:0-cer was found to be most strongly destabilizing to domains, even more so than its unsaturated counterpart. Comparison of chain-analogous ceramides and diacylglycerols in Fig. 3 shows a slightly greater propensity for diacylglycerol species to stabilize domains (compare e.g., C16:0-cer and C16:0-dag). However, introduction of a domain suppressing feature such as chain unsaturation negates the stabilizing contribution of the backbone (compare e.g., C18:1-cer and C18:1-dag).

3. Discussion

Using SANS we investigated the effect of ceramide or diacylglycerol structure on the lateral organization of phosphatidylcholine bilayers exhibiting L_d+L_o phase separation. While many studies have focused on the competition between cholesterol and ceramide in sphingomyelin-rich domains (Maula et al., 2015; Sot et al., 2008; Castro et al., 2009), we used a system of glycerophospholipids to restrict hydrogen bonding contributions (Slotte, 2016), thereby emphasizing the role of the N-acyl chain. Our baseline composition presents domains with moderate amounts of cholesterol (25 mol%) (Veatch and Keller, 2003). We observe changes in DPPC clustering at low ratios of ceramide:saturated lipid, which are devoid of gel phases owing to the cholesterol content (Castro et al., 2009). In agreement with previous studies, we find the following rank order of structural features that influence lateral organization: chain unsaturation > chain length > backbone structure.

3.1. Ceramide chain unsaturation suppresses domains

All unsaturated ceramide species studied here promote the mixing of saturated and unsaturated lipid components. Structurally, the small polar headgroups of ceramides and diacylglycerols result in conical lipid shapes that destabilize lamellar phases (Epand, 1985). Moreover, *cis*-double bonds introduce kinks in the acyl chains that further decrease molecular packing efficiency and limit van der Waals interactions between adjacent acyl chains (Marsh, 1999). Regardless, monolayer and fluorescence studies have shown that unsaturated ceramide species favorably interact with condensed phases (Wang and Silvius, 2003; Dupuy and Maggio, 2014; Maula et al., 2015; Pinto et al., 2011). As a result of their molecular structures, ceramides and diacylglycerols seek out ordered domains as a means to shelter their large hydrophobic moieties from the aqueous phase, analogous to the "umbrella model" in the case of cholesterol (Huang and Feigenson, 1999). We find that incorporation of cer or dag species containing chain unsaturations destabilizes domains, presumably by lowering domain order and thus reducing the difference in order between L_o and L_d phases.

Interestingly, at 15 °C (Fig. 3a) all of the unsaturated lipids that we studied appear to suppress lateral phase separation to approximately the same degree. As noted in previous work (Maula et al., 2015; Pinto et al., 2011), the location of the *cis*-double bond is a critical factor in determining the extent of lipid domain destabilization. As shown in Fig. 3a, comparing C6:1-cer species with equivalent chain length and unsaturation, the centralized double bond of C6:1(3)-cer destabilizes domains to a greater degree than the distal double bond of C6:1(5)-cer. This trend is recapitulated in comparison of two ω-9 fatty acid-containing ceramides, where the more centrally located double bond of C18:1-cer$^{\Delta 9c}$ abolished domains at a lower temperature than C24:1-cer$^{\Delta 15c}$ (Fig. 3b).

It has previously been shown that the highly asymmetric acyl chains of C24:1-cer can induce interdigitated phases in mixed lipid membranes (Pinto et al., 2008; Nyholm et al., 2010). Interdigitation might minimize packing constraints and stabilize domains containing long unsaturated ceramide chains. At 15 °C (Fig. 3a), all unsaturated acyl chain ceramides produce vesicles with approximately 40% of the total scattering Q of the system with no ceramide. Increasing the temperature to 25 °C (Fig. 3b) results in a lesser decrease in Q for C24:1-cer compared to the other unsaturated ceramides, suggesting a greater resistance of the C24:1-cer-containing domains to thermal disruption. Our data supports an additional contribution, such as interdigitation, as a mechanism to stabilize phases by limiting packing constraints. The effect of interdigitation is also evidenced by the greater ability of C24:1-cer to form gel domains in bilayers (Pinto et al., 2008) compared to monolayers (Dupuy and Maggio, 2014).

3.2. Ceramide chain length tunes domain stability

Earlier studies identified that trends in the membrane behavior of

ceramides are correlated with the length of their N-acyl chains, and that a matched hydrophobic thickness maximizes van der Waals interactions to stabilize gel-like phases (Carrer and Maggio, 1999; Karttunen et al., 2009). In contrast, it has also been shown that progressive chain asymmetry and mismatch of bilayer thickness decreases the miscibility transition temperature (i.e., destabilizes sterol-sphingolipid ordered domains) (Maula et al., 2015; Nybond et al., 2005). Our results align well with existing literature in identifying C16:0-cer as the most domain stabilizing ceramide species in mixtures where ordered phases are enriched in palmitoyl chains. (Pinto et al., 2011), (Pinto et al., 2013; Maula et al., 2015; Silva et al., 2007; Megha, 2004; Megha et al., 2007)

Ceramides have been shown to have a greater affinity for ordered phases than does cholesterol (Wang and Silvius, 2003; Dupuy and Maggio, 2014; Ali et al., 2006). For example, multiple studies have shown that matching N-acyl length ceramides (C16:0-cer and C18:0-cer) are able to efficiently out-compete cholesterol for association with ordered lipids (Megha, 2004; Maula et al., 2015; Sot et al., 2008; Alanko et al., 2005; Boulgaropoulos et al., 2012). Given our neutron contrast matching scheme (described in Materials and Methods), an increase in the total scattering Q can be attributed to increases in either or both of two interdependent modes: (i) a greater area fraction of ordered domains (a_d); and (ii) greater contrast ($\Delta\rho$) due to stronger partitioning of DPPC between the ordered domains and bulk disordered phase. Based on increased total scattering, our data show that these chain-matched species are most effective in promoting clustering of the saturated DPPC lipids. This stabilizing effect is very pronounced and results in the formation of ordered lipid domains in what would otherwise have been a homogeneous mixture at near-physiological temperature (Fig. 3c).

Highly asymmetric ceramide species induce disordering of saturated lipids to varying degrees. Very long-chain ceramides (C24:0-cer) possesses a strong negative curvature and the ability to interdigitate. These features can promote tubule formation at high ceramide concentrations (Pinto et al., 2011; Levin et al., 1985; Jiménez-Rojo et al., 2014), though we do not observe any evidence of tubulation at 10 mol% ceramide. As a consequence of their ability to perturb molecular packing, condensed phases composed of very long-chain ceramides are less ordered and exhibit complex melting behavior (Maula et al., 2015). At a 1:1 stoichiometry of saturated lipid:ceramide and 10 mol% cholesterol, (Maula et al., 2015) found that C24:0-cer promotes membrane order, albeit less so compared to C16:0-cer or C18:0-cer (Maula et al., 2015). In the current study, we used a higher proportion of saturated lipid and cholesterol (a saturated lipid:ceramide molar ratio of 2.75:1 and 25 mol % cholesterol) and found that C24:0-cer destabilizes saturated lipid clusters. The discrepancy between this and previous results can be rationalized by the lower capacity of POPC/PSM/Chol/Cer (60/15/10/15) to shelter ceramide from the aqueous phase, compared to DOPC/DPPC/Chol/Cer (37.5/27.5/25/10). The limited shielding capacity of the former mixture forces a closer association between the ceramide and saturated lipid. We further note that of all the lipid species we identified as destabilizing lipid domains (i.e., those beneath the horizontal line in Fig. 3), the composition with C24:0-cer was the least responsive to temperature. Although C24:0-cer decreases the ability of DPPC to cluster, the ordered phase that it forms is rather stable, possibly due to its ability to interdigitate (Levin et al., 1985).

Short chain ceramides are known to have a significant disordering effect on biological membranes and are not known to induce acyl chain interdigitation. Our work closely mirrors that of (Megha et al., 2007), which studied the behavior of ceramides in brain sphingomyelin and reached similar conclusions regarding the influence of short-chain ceramides on domain stability. Though that study used a larger ceramide mole fraction (18 mol%, compared to 10 mol% in the present study), the authors observed a slightly destabilizing effect on lipid rafts upon incorporation of C12:0-cer, which they attributed to the ability of the ceramide to displace cholesterol (Megha et al., 2007). Additionally, Megha et al. (2007) found C6:0-cer to be among the lipids with the greatest ability to destabilize ordered lipid domains, in agreement with the work of Nybond et al. (2005) and our findings (Nybond et al., 2005). Domain disordering by short-chain ceramides has been suggested to arise from perturbations to interfacial lipid packing caused by the short acyl chain (Nybond et al., 2005). Our results show that these short chain species do not provide sufficient favorable interactions to stabilize ordered phases and thus result in significant membrane disorder, with C6:0-cer being the most domain destabilizing lipid of those studied here. Several studies have shown that C6:0-cer is also the most apoptotic ceramide species, which may be a consequence of this destabilization (Brown et al., 1999; Ogretmen, 2018; Kester et al., 2015; Shaw et al., 2018).

Work by Megha (2004) suggested a limited capacity of ordered phases to accommodate small-headgroup ceramide species (Megha, 2004; Ali et al., 2006). This solubility limit results in a competition between cholesterol and ceramide that leads to the most favorable association, i.e., a gel phase enriched in ceramide and saturated lipid (Ali et al., 2006). The extent of the competition depends on the relative amounts of ceramide/cholesterol and the saturated lipid species. When the saturated lipid is in limited supply, even small amounts of ceramide are observed to displace cholesterol from ordered domains (Silva et al., 2007; Castro et al., 2009; Boulgaropoulos et al., 2012). In biological membranes, the displaced cholesterol can be removed from the bilayer through various pathways (Lange and Steck, 2008). However, at fixed lipid compositions such as those found in model membrane studies, cholesterol is released and is then able to nucleate a liquid-ordered phase domain (Megha, 2004; Boulgaropoulos et al., 2012). Indeed, the formation of ceramide-rich gel domains surrounded by a cholesterol-rich liquid-ordered phase has been inferred from FRET and fluorescence anisotropy data (Silva et al., 2007; Pinto et al., 2013; Chiantia et al., 2006). Alternatively, at intermediate cholesterol concentrations and with an abundance of saturated lipid (such as in this work), competition between cholesterol and ceramide results in the formation of an ordered phase composed primarily of saturated lipid, cholesterol, and ceramide (Busto et al., 2010), (Busto et al., 2014; Maula et al., 2015; Nyholm et al., 2010). This heterogeneous ordered phase may have unique physicochemical properties as it teeters between a cholesterol-rich (L_o, no long range order) and a ceramide-rich (L_β, long range order) phase (Silva et al., 2009; García-Arribas et al., 2015), (García-Arribas et al., 2016; Megha, 2004). Future studies probing the physical properties of heterogeneous domains may be able to comment on the ability of cholesterol:ceramide mixtures to tune membrane biophysical properties.

3.3. *Backbone structure is a secondary factor*

Ceramide and diacylglycerol are structurally similar; most notably, both possess a small polar headgroup. With their sphingosine backbone, ceramides are capable of both donating and accepting hydrogen bonds, in contrast to glycerides that can only accept hydrogen bonds. It is known that sphingolipid-rich condensed phases benefit from an inter- and intra-molecular hydrogen bonding network that is coordinated by the C4 *trans*-double bond of the base (Li et al., 2001; Jaikishan and Slotte, 2013; Löfgren and Pascher, 1977; Brockman et al., 2004). This suggests that ceramide's ability to form hydrogen bonds promotes the formation and stabilization of ceramide-rich platforms in sphingolipid mixtures.

From Fig. 3, a comparison of C16:0-dag to C16:0-cer in the absence of sphingomyelin shows that clustering of DPPC is enhanced by chain-equivalent diacylglycerols, compared to ceramides. However, the domain-enhancing feature offered by the diacylglycerol backbone is more than offset by the penalty of chain unsaturation (compare C18:1-dag to C18:1-cer in Fig. 3). This is in agreement with the findings of Megha (2004), who showed that C16:0-dag is most efficient in displacing cholesterol from ordered bilayers due to its enhanced packing efficiency (Megha, 2004). In addition, investigations by Sot et al. (2008) indicate that natural extracts of egg diacylglycerols destabilize

sphingomylein-rich phases, while egg ceramide is stabilizing (Sot et al., 2008). In agreement with our data and the findings of others, it is likely that this observation is a result of the greater amount of saturated acyl chains in the ceramide extract (60%), compared to the diacylglycerol extract (40%), rather than a preference for one backbone structure over the other.

Maula et al. (2015) characterized the influence of phytosphingosine and 2′-hydroxyceramide species on phase separation. In a sphingolipid-rich system, they determined that the additional hydroxyl group increases domain stability due to greater hydrogen bonding. However, elimination of the C4 *trans*-double bond in phytosphingosine and additional steric contributions from the -OH group, prevents the tight packing necessary for condensed phases (Maula et al., 2015). Based on the structure of diacylglycerol, which is devoid of hydrogen bond donors, it is reasonable to attribute its affinity for glycerophospholipid phases largely to its structural similarity (and therefore favorability to pack) as compared to ceramide. Still, further investigations are warranted to explore the phase behavior of various diacylglycerol species in a sphingolipid-containing raft-mimicking composition to better compare the influence of hydrogen bonding and backbone structure.

4. Conclusions

Using SANS from lipid vesicles that are models for membrane rafts, we observe differences in lipid clustering in the presence of ceramides and diacylglycerols of varying chain length and unsaturation. From the data we draw two main conclusions: (1) C16:0 and C18:0 ceramides stabilize ordered domains, in contrast to the destabilizing effect manifested by short (C6:0) or very long (C24:0) ceramides; and (2) monosaturated ceramides of any chain length destabilize lipid clustering. Although the molecular structure of the lipid backbone and its hydrogen bonding abilities further stabilize lipid domains, its role is of lesser consequence. Our findings can be explained by a competition between cholesterol and ceramide in seeking shelter from the aqueous phase, thus producing domains that bridge the physicochemical properties of the gel- and liquid-ordered phases.

5. Experimental

5.1. Materials

Lipids and cholesterol were dissolved in HPLC-grade chloroform to a known concentration and stored at - 80 ˚C. Ultrapure H_2O was obtained from a High-Q purification system (Wilmette, IL) and D_2O (99.9%) was purchased from Cambridge Isotopes (Andover, MA). Cholesterol was from Nu-Chek Prep (Elysian, MN). 1,2-dipalmitoyl-*sn*-glycero-3-phosphocholine (DPPC), 1,2-dioleoyl-*sn*-glycero-3-phosphocholine (DOPC), 1,2-dipalmitoyl-*sn*-glycerol (C16:0-diacylglycerol, C16:0-dag), 1-palmitoyl-2-oleoyl-*sn*-glycerol (C18:1-diacylglycerol, C18:1-dag), *N*-hexanoyl-D-*erythro*-spingosine (C6:0-ceramide, C6:0-cer), *N*-lauroyl-D-*erythro*-spingosine (C12:0-ceramide, C12:0-cer), *N*-palmitoyl-D-*erythro*-spingosine (C16:0-ceramide, C16:0-cer), *N*-stearoyl-D-*erythro*-spingosine (C18:0-ceramide, C18:0-cer), *N*-oleoyl-D-*erythro*-spingosine (C18:1-ceramide, C18:1-cer), *N*-lignoceroyl-D-*erythro*-spingosine (C24:0-ceramide, C24:0-cer), and *N*-nervonoyl-D-*erythro*-spingosine (C24:1-ceramide, C24:1-cer) were purchased from Avanti Polar Lipids (Alabaster, AL) and used as supplied.

N-hex-3-enoyl-D-*erythro*-sphingosine (**5**) and *N*-hex-5-enoyl-D-*erythro*-sphingosine (**7**) were prepared according to the synthetic steps outlined in Scheme 4 following literature methods (Szulc et al., 2010; Camacho et al., 2013). Briefly, D-sphingosine (**1**) was converted to corresponding acetonide **3** by treating with 2-methoxy-1-propene (**2**) in the presence of a catalytic amount of pyridinium *p*-toluenesulfonate (PPTS) in refluxing toluene for 4 h (Szulc et al., 2010). The resulting D-sphingosine acetonide **3** and Et_3N in CH_3CN, on treatment with a solution of 1-hydroxybenzotriazole monohydrate ($HOBt{\cdot}H_2O$), *trans*-3-hexenoic acid or 5-hexenoic acid, and *N*-(3-dimethylaminopropyl)-*N*′-ethylcarbodiimide hydrochloride (EDCI.HCl) in CH_2Cl_2 at room temperature for 1 h resulted in the corresponding acetonide protected C6-ceramide analogs **4** and **6** in 72% and 75% yields, respectively (Camacho et al., 2013). Compounds **4** and **6** on reaction with catalytic amount of *p*-toluenesulfonic acid (PTSA) in MeOH at room temperature for 2 h afforded the corresponding *N*-hex-3-enoyl-D-*erythro*-sphingosine (**5**) and *N*-hex-5-enoyl-D-*erythro*-sphingosine (**7**), respectively, in quantitative yields (Szulc et al., 2010). Both the compounds **5** and **7** were characterized on the basis of NMR and MS spectral data (DNS).

5.2. Preparation of LUVs for small-angle neutron scattering (SANS)

Large unilamellar vesicle (LUV) samples for SANS measurements were prepared as follows. Desired volumes of lipid and cholesterol stock solutions in chloroform were transferred to a glass vial using a glass syringe. Organic solvent was removed under a nitrogen stream with mild heating. Lipid films were then placed under vacuum for >12 h to remove trace solvent. Dry lipid films were hydrated with a 34.5% (v/v) D_2O/H_2O mixture preheated to 45 ˚C and subsequently vortexed to generate multilamellar vesicles (MLVs). The MLV suspension was incubated at 45 ˚C for 1 h, followed by 5 freeze/thaw cycles between - 80 and 45 ˚C. Samples were then sonicated at 60 ˚C for 1 min. Unilamellar liposomes were prepared using a miniextruder (Avanti Polar Lipids, Alabaster, AL) assembled with a single 50 nm diameter pore size polycarbonate filter and heated to 45 ˚C. Final sample concentrations were 10–20 mg/mL, allowing for sufficient water between vesicles to eliminate the interparticle structure factor. The resulting vesicles had an average diameter of 90 ± 10 nm as determined by dynamic light scattering.

5.3. SANS data collection

SANS experiments were conducted at the High Flux Isotope Reactor (HFIR) of the Oak Ridge National Laboratory (ORNL) using the CG-3 BioSANS instrument (Heller et al., 2018). LUV suspensions were loaded into 1 mm path-length quartz cylindrical cells (Hellma USA, Plainview, NY) and mounted in a temperature-controlled holder with $\pm$ 1 ˚C accuracy. Scattered neutrons were counted with ^{3}He linear position-sensitive detector tubes (GE Reuter Stokes, Twinsburg, OH) assembled to form a 1×1 m (192×256 pixels) main detector, and a 1×0.8 m (160×256 pixels) curved wide-angle “wing” detector. SANS data were collected with a single instrument configuration covering a total scattering range of $0.003 < q < 0.8$ Å^{-1} using 6 Å wavelength neutrons (FWHM 15%) with the main and wing detectors at sample-to-detector distances of 15.5 m and 1.13 m, respectively. The tube closest to the beam of the wing detector was rotated out of the primary beam path by 1.4˚. Neutron beam collimation was defined by source and sample apertures (40 and 14 mm diameter, respectively) placed 17.5 m apart. No neutron guides or attenuators were used. The 2D data were reduced and combined using the Mantid software package (Arnold et al., 2014). Data were corrected for detector pixel sensitivity, dark current and sample transmission, as well as background scattering from water. Reduced 2D data sets were azimuthally averaged to obtain 1D SANS profiles of scattering intensity I vs. wavevector q, where q is a function of the neutron wavelength λ and scattering angle 2θ through the relationship $q = 4\pi \sin\theta/\lambda$.

5.4. SANS analysis

Data backgrounds were normalized by subtracting the slope of $I(q) \times q^4$ vs. q^4 for $q > 0.6$ Å^{-1} from the data to correct for sample-to-sample variation in the flat incoherent background (Porod, 1951; Alava et al., 2002). Following Pencer et al. (2006) data were then analyzed as model-independent quantities through the Porod invariant, Q:

$$Q = \int I(q)q^2 dq \quad (1)$$

To a first approximation, Q is related to the degree of phase separation and the difference in neutron scattering length density (i.e., the contrast) between the two phases as:

$$Q \approx a_d(1 - a_d)\Delta\rho^2, \quad (2)$$

where a_d and (1 - a_d) are the area fractions occupied by the domain and matrix phases, respectively, and $\Delta\rho$ is the contrast between the phases. The resulting Porod invariants were normalized as a fraction of the invariant of the non-doped lipid mixture at 15 °C, where phase separation is understood to be most robust.

Contributions

Conceived the project: M.K., J.K., F.A.H., T.G.D. Designed the experiments: F.A.H., T.G.D., D.M., M.K., J.K. Performed experiments: F.A.H., T.G.D., D.M., M.D., T.E.F. Analyzed data: F.A.H., D.M., M.D. Synthesized reagents: A.S.K., S.A., D.D. Drafted the manuscript: M.D., D.M., F.A.H. Revised the manuscript for intellectual content: M.D., D.M., F.A.H., M.K., J.K.

Declaration of Competing Interest

Penn State Research Foundation has licensed ceramide nanoliposome technology to Keystone Nano, Inc. (Pennsylvania). M.K. is CTO and co-founder of Keystone Nano.

Acknowledgements

F.A.H. is supported by NSF grant MCB-1817929 and NIH/National Institute of General Medical Sciences grant R01GM138887. D.M. is supported by Natural Science and Engineering Council of Canada (NSERC) funding reference number RGPIN-2018-04841. M.K. is supported by NIH grant 5P01 CA 171983–07. J.K. is supported by the Scientific User Facilities Division of the Department of Energy (DOE) Office of Science, sponsored by the Basic Energy Science (BES) Program, DOE Office of Science, under Contract No. DEAC05-00OR22725. A portion of this research used resources at the High Flux Isotope Reactor and the Physical Characterization Suite of the Shull Wollan Center, DOE Office of Science User Facilities operated by Oak Ridge National Laboratory.

References

Ackerman, D.G., Heberle, F.A., Feigenson, G.W., 2013. Limited perturbation of a DPPC bilayer by fluorescent lipid probes: a molecular dynamics study. J. Phys. Chem. B 117, 4844–4852. https://doi.org/10.1021/jp400289d.

Alanko, S.M., Halling, K.K., Maunula, S., Slotte, J.P., Ramstedt, B., 2005. Displacement of sterols from sterol/sphingomyelin domains in fluid bilayer membranes by competing molecules. Biochim. Biophys. Acta ((BBA)) - Biomembr. 1715, 111–121. https://doi.org/10.1016/j.bbamem.2005.08.002.

Alava, C., Arrighi, V., Cameron, J.D., Cowie, J.M.G., Moeller, A., Triolo, A., Vaqueiro, P., 2002. SANS studies of solutions and molecular composites prepared from cellulose tricarbanilate. Appl. Phys. A: Mater. Sci. Process. 74, 472–475. https://doi.org/10.1007/s003390201522.

Ali, M.R., Cheng, K.H., Huang, J., 2006. Ceramide drives cholesterol out of the ordered lipid bilayer phase into the crystal phase in 1-palmitoyl-2-oleoyl-sn-glycero-3-phosphocholine/cholesterol/ceramide ternary mixtures. Biochemistry 45, 12629–12638. https://doi.org/10.1021/bi060610x.

Allender, D., Giang, H., Schick, M., 2020. Model plasma membrane exhibits a microemulsion in both leaves providing a foundation for “rafts". Biophys. J. 118, 1019–1031.

Arnold, O., Bilheux, J.C., Borreguero, J.M., Buts, A., Campbell, S.I., Chapon, L., Doucet, M., Draper, N., FerrazLeal, R., Gigg, M.A., Lynch, V.E., Markvardsen, A., Mikkelson, D.J., Mikkelson, R.L., Miller, R., Palmen, K., Parker, P., Passos, G., Perring, T.G., Peterson, P.F., Ren, S., Reuter, M.A., Savici, A.T., Taylor, J.W., Taylor, R.J., Tolchenov, R., Zhou, W., Zikovsky, J., 2014. Mantid - data analysis and visualization package for neutron scattering and μ SR experiments. Nucl. Instrum. Methods Phys. Res. Sect. A: Accel. Spectrom. Detect. Assoc. Equip. 764, 156–166. https://doi.org/10.1016/j.nima.2014.07.029.

Boulgaropoulos, B., Rappolt, M., Sartori, B., Amenitsch, H., Pabst, G., 2012. Lipid sorting by ceramide and the consequences for membrane proteins. Biophys. J. 102, 2031–2038. https://doi.org/10.1016/j.bpj.2012.03.059.

Brockman, H.L., Momsen, M.M., Brown, R.E., He, L., Chun, J., Byun, H.-S., Bittman, R., 2004. The 4,5-double bond of ceramide regulates its dipole potential, elastic properties, and packing behavior. Biophys. J. 87, 1722–1731. https://doi.org/10.1529/biophysj.104.044529.

Brown, G.C., Nicholls, D.G., Cooper, C.E., Richter, C., Ghafourifar, P., 1999. Ceramide induces cytochrome c release from isolated mitochondria. Biochem. Soc. Symp. 66, 27–31. https://doi.org/10.1042/bss0660027.

Busto, J.V., Sot, J., Requejo-Isidro, J., Goñi, F.M., Alonso, A., 2010. Cholesterol displaces palmitoylceramide from its tight packing with palmitoylsphingomyelin in the absence of a liquid-disordered phase. Biophys. J. 99, 1119–1128. https://doi.org/10.1016/j.bpj.2010.05.032.

Busto, J.V., Garcìa-Arribas, A.B., Sot, J., Torrecillas, A., Gómez-Fernández, J.C., Goñi, F.M., Alonso, A., 2014. Lamellar gel (l_{β}) phases of ternary lipid composition containing ceramide and cholesterol. Biophys. J. 106, 621–630. https://doi.org/10.1016/j.bpj.2013.12.021.

Camacho, L., Meca-Cortés, O., Abad, J.L., García, S., Rubio, N., Díaz, A., Celià-Terrassa, T., Cingolani, F., Bermudo, R., Fernández, P.L., Blanco, J., Delgado, A., Casas, J., Fabriàs, G., Thomson, T.M., 2013. Acid ceramidase as a therapeutic target in metastatic prostate cancer. J. Lipid Res. 54, 1207–1220. https://doi.org/10.1194/jlr.M032375.

Carrer, D.C., Maggio, B., 1999. Phase behavior and molecular interactions in mixtures of ceramide with dipalmitoylphosphatidylcholine. J. Lipid Res. 40, 1987–1989. https://doi.org/10.1016/S0022-2275(20)32421-4.

Castro, B.M., Silva, L.C., Fedorov, A., de Almeida, R.F., Prieto, M., 2009. Cholesterol-rich fluid membranes solubilize ceramide domains: implications for the structure and dynamics of mammalian intracellular and plasma membranes. J. Biol. Chem. 284, 22978–22987. https://doi.org/10.1074/jbc.M109.026567.

Chiantia, S., Kahya, N., Ries, J., Schwille, P., 2006. Effects of ceramide on liquid-ordered domains investigated by simultaneous afm and fcs. Biophys. J. 90, 4500–4508. https://doi.org/10.1529/biophysj.106.081026.

Cremesti, A.E., Goñi, F.M., Kolesnick, R.N., 2002. Role of sphingomyelinase and ceramide in modulating rafts: do biophysical properties determine biologic outcome? FEBS Lett. 531, 47–53. https://doi.org/10.1016/S0014-5793(02)03489-0.

Dupuy, F.G., Maggio, B., 2014. N-acyl chain in ceramide and sphingomyelin determines their mixing behavior, phase state, and surface topography in langmuir films. J. Phys. Chem. B 118, 7475–7487. https://doi.org/10.1021/jp501686q.

Epand, R.M., 1985. Diacylglycerols, lysolecithin, or hydrocarbons markedly alter the bilayer to hexagonal phase transition temperature of phosphatidylethanolamines. Biochemistry 24, 7092–7095. https://doi.org/10.1021/bi00346a011.

Feigenson, G., 1863. On the small size of liquid-disordered. liquid-ordered nanodomains. Biochim. Biophys. Acta 2021, 183685.

García-Arribas, A.B., Alonso, A., Goñi, F.M., 2016. Cholesterol interactions with ceramide and sphingomyelin. Chem. Phys. Lipids 199, 26–34. https://doi.org/10.1016/j.chemphyslip.2016.04.002 (properties and Functions of Cholesterol).

García-Arribas, A.B., Busto, J.V., Alonso, A., Goñi, F.M., 2015. Atomic force microscopy characterization of palmitoylceramide and cholesterol effects on phospholipid bilayers: A topographic and nanomechanical study. Langmuir 31, 3135–3145. https://doi.org/10.1021/la504047n pMID: 25693914.

Goñi, F.M., Alonso, A., 2009. Effects of ceramide and other simple sphingolipids on membrane lateral structure. Biochim. Biophys. Acta ((BBA)) - Biomembr. 1788, 169–177. https://doi.org/10.1016/j.bbamem.2008.09.002.

Grassmé, H., Jendrossek, V., Bock, J., Riehle, A., Gulbins, E., 2002. Ceramide-rich membrane rafts mediate cd40 clustering. J. Immunol. 168, 298–307. https://doi.org/10.4049/jimmunol.168.1.298.

Hannun, Y.A., 1996. Functions of ceramide in coordinating cellular responses to stress. Science 274, 1855–1859. https://doi.org/10.1126/science.274.5294.1855.

Heberle, F., Feigenson, G., 2011. Phase separation in lipid membranes. Cold Spring Harbor Perspect. Biol. 3, a004630.

Heberle, F.A., Petruzielo, R.S., Pan, J., Drazba, P., Kučerka, N., Standaert, R.F., Feigenson, G.W., Katsaras, J., 2013. Bilayer thickness mismatch controls domain size in model membranes. J. Am. Chem. Soc. 135, 6853–6859. https://doi.org/10.1021/ja3113615.

Heller, W.T., Cuneo, M., Debeer-Schmitt, L., Do, C., He, L., Heroux, L., Littrell, K., Pingali, S.V., Qian, S., Stanley, C., Urban, V.S., Wu, B., Bras, W., 2018. The suite of small-angle neutron scattering instruments at Oak Ridge National Laboratory. J. Appl. Crystallogr. 51, 242–248. https://doi.org/10.1107/S1600576718001231.

Huang, J., Feigenson, G.W., 1999. A microscopic interaction model of maximum solubility of cholesterol in lipid bilayers. Biophys. J. 76, 2142–2157. https://doi.org/10.1016/S0006-3495(99)77369-8.

Huang, W.-C., Chen, C.-L., Lin, Y.-S., Lin, C.-F., 2011. Apoptotic sphingolipid ceramide in cancer therapy. J. Lipids 2011, 1–15. https://doi.org/10.1155/2011/565316.

Ipsen, J., Karlstrom, G., Mouritsen, O., Wennerstrom, H., Zuckermann, M., 1987. Phase equilibria in the phosphatidylcholine-cholesterol system. Biochim. Biophys. Acta 905, 162–172. https://doi.org/10.1016/0005-2736(87)90020-4.

Jaikishan, S., Slotte, J.P., 2013. Stabilization of sphingomyelin interactions by interfacial hydroxyls - a study of phytosphingomyelin properties. Biochim. Biophys. Acta ((BBA)) - Biomembr. 1828, 391–397. https://doi.org/10.1016/j.bbamem.2012.08.029.

Jiménez-Rojo, N., García-Arribas, A.B., Sot, J., Alonso, A., Goñi, F.M., 2014. Lipid bilayers containing sphingomyelins and ceramides of varying n-acyl lengths: a glimpse into sphingolipid complexity. Biochim. Biophys. Acta ((BBA)) - Biomembr. 1838, 456–464. https://doi.org/10.1016/j.bbamem.2013.10.010.

Karttunen, M., Haataja, M.P., Säily, M., Vattulainen, I., Holopainen, J.M., 2009. Lipid domain morphologies in phosphatidylcholines-ceramide monolayers. Langmuir 25, 4595–4600. https://doi.org/10.1021/la803377s.

Kester, M., Bassler, J., Fox, T.E., Carter, C.J., Davidson, J.A., Parette, M.R., 2015. Preclinical development of a c6-ceramide nanoliposome, a novel sphingolipid therapeutic. Biol. Chem. 396, 737–747. https://doi.org/10.1515/hsz-2015-0129.

Kinnunen, P.K.J., Kõiv, A., Lehtonen, J.Y.A., Rytömaa, M., Mustonen, P., 1994. Lipid dynamics and peripheral interactions of proteins with membrane surfaces. Chem. Phys. Lipids 73, 181–207. https://doi.org/10.1016/0009-3084(94)90181-3 (special Issue Functional Dynamics of Lipids in Biomembranes).

Kolesnick, R.N., Goñi, F.M., Alonso, A., 2000. Compartmentalization of ceramide signaling: physical foundations and biological effects. J. Cell. Physiol. 184, 285–300, 10.1002/1097-4652(200009)184:3<285::AID-JCP2>3.0.CO;2-3.

Lange, Y., Steck, T.L., 2008. Cholesterol homeostasis and the escape tendency (activity) of plasma membrane cholesterol. Prog. Lipid Res. 47, 319–332. https://doi.org/10.1016/j.plipres.2008.03.001.

Laviad, E.L., Albee, L., Pankova-Kholmyansky, I., Epstein, S., Park, H., Jr, A.H.M., Futerman, A.H., 2008. Characterization of ceramide synthase 2 tissue distribution, substrate specificity, and inhibition by sphingosine-1-phosphate. Lipids Lipoproteins 283, 5677–5684. https://doi.org/10.1074/jbc.M707386200.

Levental, I., Levental, K., Heberle, F., 2020. Lipid rafts: controversies resolved, mysteries remain. Trends Cell Biol. 30, 341–353. https://doi.org/10.1016/j.tcb.2020.01.009.

Levin, I.W., Thompson, T.E., Barenholz, Y., Huang, C., 1985. Two types of hydrocarbon chain interdigitation in sphingomyelin bilayers. Biochemistry 24, 6282–6286. https://doi.org/10.1021/bi00343a036.

Li, X.-M., Momsen, M.M., Smaby, J.M., Brockman, H.L., Brown, R.E., 2001. Cholesterol decreases the interfacial elasticity and detergent solubility of sphingomyelins. Biochemistry 40, 5954–5963. https://doi.org/10.1021/bi002791n.

Li, Y.C., Park, M.J., Ye, S.-K., Kim, C.-W., Kim, Y.-N., 2006. Elevated levels of cholesterol-rich lipid rafts in cancer cells are correlated with apoptosis sensitivity induced by cholesterol-depleting agents. Am. J. Pathol. 168, 1107–1118. https://doi.org/10.2353/ajpath.2006.050959.

Löfgren, H., Pascher, I., 1977. Molecular arrangements of sphingolipids. the monolayer behaviour of ceramides. Chem. Phys. Lipids 20, 273–284. https://doi.org/10.1016/0009-3084(77)90068-8.

Marsh, D., 1788. Cholesterol-induced fluid membrane domains: a compendium of lipid-raft ternary phase diagrams. Biochim. Biophys. Acta 2009, 2114–2123.

Marsh, D., 1999. Thermodynamic analysis of chain-melting transition temperatures for monounsaturated phospholipid membranes: dependence on cis-monoenoic double bond position. Biophys. J. 77, 953–963. https://doi.org/10.1016/S0006-3495(99)76946-8. ⟨https://www.sciencedirect.com/science/article/pii/S0006349599769468⟩.

Mathias, S., Peña, L.A., Kolesnick, R.N., 1998. Signal transduction of stress via ceramide. Biochem. J. 335, 465–480. https://doi.org/10.1042/bj3350465.

Maula, T., AlSazzad, M., Slotte, J., 2015. Influence of hydroxylation, chain length, and chain unsaturation on bilayer properties of ceramides. Biophys. J. 109, 1639–1651. https://doi.org/10.1016/j.bpj.2015.08.040.

Megha, E. London, 2004. Ceramide selectively displaces cholesterol from ordered lipid domains (rafts): Implications for lipid raft structure and function. J. Biol. Chem. 279, 9997–10004. https://doi.org/10.1074/jbc.M309992200. ⟨https://www.sciencedirect.com/science/article/pii/S0021925817476496⟩.

Megha, P., Sawatzki, T., Kolter, R., Bittman, E., 2007. London, Effect of ceramide n-acyl chain and polar headgroup structure on the properties of ordered lipid domains (lipid rafts). Biochim. Biophys. Acta ((BBA)) - Biomembr. 1768, 2205–2212. https://doi.org/10.1016/j.bbamem.2007.05.007.

Nybond, S., Björkqvist, Y.J.E., Ramstedt, B., Slotte, J.P., 2005. Acyl chain length affects ceramide action on sterol/sphingomyelin-rich domains. Biochim. Biophys. Acta ((BBA)) - Biomembr. 1718, 61–66. https://doi.org/10.1016/j.bbamem.2005.10.009.

Nyholm, T.K.M., Grandell, P.-M., Westerlund, B., Slotte, J.P., 2010. Sterol affinity for bilayer membranes is affected by their ceramide content and the ceramide chain length. Biochim. Biophys. Acta ((BBA)) - Biomembr. 1798, 1008–1013. https://doi.org/10.1016/j.bbamem.2009.12.025.

Ogretmen, B., 2018. Sphingolipid metabolism in cancer signalling and therapy. Nat. Rev. Cancer 18, 33–50. https://doi.org/10.1038/nrc.2017.96.

Pencer, J., Anghel, V.N., Kučerka, N., Katsaras, J., 2006. Scattering from laterally heterogeneous vesicles. I. Model-independent analysis. J. Appl. Crystallogr. 39, 791–796. https://doi.org/10.1107/S0021889806035163.

Pencer, J., Mills, T.T., Kucerka, N., Nieh, M.-P., Katsaras, J., 2007. Small-angle neutron scattering to detect rafts and lipid domains. In: Lipid Rafts. Springer, pp. 231–244.

Pencer, J., Mills, T., Anghel, V., Krueger, S., Epand, R.M., Katsaras, J., 2005. Detection of submicron-sized raft-like domains in membranes by small-angle neutron scattering. Eur. Phys. J. E 18, 447–458. https://doi.org/10.1140/epje/e2005-00046-5.

Pinto, S.N., Silva, L.C., de Almeida, R.F., Preito, M., 2008. Membrane domain formation, interdigitation, and morphological alterations induced by the very long chain asymmetric c24:1 ceramide. Biophys. J. 95, 2867–27879. https://doi.org/10.1529/biophysj.108.129858.

Pinto, S.N., Silva, L.C., Futerman, A.H., Preito, M., 2011. Effect of ceramide structure on membrane biophysical properties: the role of acyl chain length and unsaturation. Biochim. Biophys. Acta ((BBA)) - Biomembr. 1808, 2753–2760. https://doi.org/10.1016/j.bbamem.2011.07.023.

Pinto, S.N., Fernandes, F., Fedorov, A., Futerman, A.H., Silva, L.C., Prieto, M., 2013. A combined fluorescence spectroscopy, confocal and 2-photon microscopy approach to re-evaluate the properties of sphingolipid domains. Biochim. Biophys. Acta ((BBA)) - Biomembr. 1828, 2099–2110. https://doi.org/10.1016/j.bbamem.2013.05.011. ⟨http://www.sciencedirect.com/science/article/pii/S0005273613001570⟩.

Porod, G., 1951. Die Röntgenkleinwinkelstreuung von dichtgepackten kolloiden Systemen. Kolloid-Zeitschrift 124, 83–114. https://doi.org/10.1007/BF01512792.

Pushkareva, M., Obeid, L.M., Hannun, Y.A., 1995. Ceramide: an endogenous regulator of apoptosis and growth suppression. Immunol. Today 16, 294–297. https://doi.org/10.1016/0167-5699(95)80184-7.

Shaw, J., Costa-Pinheiro, P., Patterson, L., Drews, K., Spiegel, S., Kester, M., 2018. Chapter twelve – novel sphingolipid-based cancer therapeutics in the personalized medicine era. In: Chalfant, C.E., Fisher, P.B. (Eds.), Sphingolipids in Cancer, volume 140 of Advances in Cancer Research. Academic Press, pp. 327–366. https://doi.org/10.1016/bs.acr.2018.04.016.

Silva, L.C., Futerman, A.H., Prieto, M., 2009. Lipid raft composition modulates sphingomyelinase activity and ceramide-induced membrane physical alterations. Biophys. J. 96, 3210–3222. https://doi.org/10.1016/j.bpj.2008.12.3923.

Silva, L.C., de Almeida, R.F., Castro, B.M., Fedorov, A., Prieto, M., 2007. Ceramide-domain formation and collapse in lipid rafts: membrane reorganization by an apoptotic lipid. Biophys. J. 92, 502–516. https://doi.org/10.1529/biophysj.106.091876.

Simons, K., Ikonen, E., 1997. Functional rafts in cell membranes. Nature 387, 569–572. https://doi.org/10.1038/42408.

Slotte, J.P., 2016. The importance of hydrogen bonding in sphingomyelin's membrane interactions with co-lipids. Biochim. Biophys. Acta ((BBA)) - Biomembr. 1858, 304–310. https://doi.org/10.1016/j.bbamem.2015.12.008. ⟨https://www.sciencedirect.com/science/article/pii/S000527361500406X⟩.

Sodt, A., Pastor, R., Lyman, E., 2015. Hexagonal substructure and hydrogen bonding in liquid-ordered phases containing palmitoyl sphingomyelin. Biophys. J. 109, 948–955.

Sot, J., Ibarguren, M., Busto, J.V., Montes, L.-R., Goñi, F.M., Alonso, A., 2008. Cholesterol displacement by ceramide in sphingomyelin-containing liquid-ordered domains, and generation of gel regions in giant lipidic vesicles. FEBS Lett. 582, 3230–3236. https://doi.org/10.1016/j.febslet.2008.08.016. ⟨https://febs.onlinelibrary.wiley.com/doi/abs/10.1016/j.febslet.2008.08.016⟩.

Stancevic, B., Kolesnick, R.N., 2010. Ceramide-rich platforms in transmembrane signaling. FEBS Lett. 584, 1728–1740. https://doi.org/10.1016/j.febslet.2010.02.026 (frontiers in Membrane Biochemistry).

Szulc, Z.M., Bai, A., Bielawski, J., Mayroo, N., Miller, D.E., Gracz, H., Hannun, Y.A., Bielawska, A., 2010. Synthesis, NMR characterization and divergent biological actions of 2′-hydroxy-ceramide/dihydroceramide stereoisomers in mcf7 cells. Bioorg. Med. Chem. 18, 7565–7579. https://doi.org/10.1016/j.bmc.2010.08.050.

Veatch, S., 2022. From small fluctuations to large-scale phase separation: lateral organization in model membranes containing cholesterol. Sem. Cell Dev. Biol. 18 (207), 573–582.

Veatch, S.L., Keller, S.L., 2003. Separation of liquid phases in giant vesicles of ternary mixtures of phospholipids and cholesterol. Biophys. J. 85, 3074–3083. https://doi.org/10.1016/S0006-3495(03)74726-2.

Wang, T.-Y., Silvius, J.R., 2003. Sphingolipid partitioning into ordered domains in cholesterol-free and cholesterol-containing lipid bilayers. Biophys. J. 84, 367–378. https://doi.org/10.1016/S0006-3495(03)74857-7.

Zhang, Y., Li, X., Becke, K.A., Gulbins, E., 2009. Ceramide-enriched membrane domains - structure and function. Biochim. Biophys. Acta ((BBA)) - Biomembr. 1788, 178–183. https://doi.org/10.1016/j.bbamem.2008.07.030.